

Application of Brazilian pine-fruit shell as a biosorbent to removal of reactive red 194 textile dye from aqueous solution

Kinetics and equilibrium study

Eder C. Lima^{a,*}, Betina Royer^a, Julio C.P. Vaghetti^a, Nathalia M. Simon^a, Bruna M. da Cunha^a, Flavio A. Pavan^a, Edilson V. Benvenuti^a, Renato Cataluña-Veses^a, Claudio Airoidi^b

^a Instituto de Química, Universidade Federal do Rio Grande do Sul, Av. Bento Gonçalves 9500, Caixa Postal 15003, CEP 91501-970, Porto Alegre, RS, Brazil

^b Instituto de Química, Universidade Estadual de Campinas (UNICAMP), Campinas, SP, Brazil

Received 18 June 2007; received in revised form 22 October 2007; accepted 23 November 2007

Available online 4 December 2007

Abstract

The Brazilian pine-fruit shell (*Araucaria angustifolia*) is a food residue, that was used as biosorbent for the removal of non-hydrolyzed reactive red 194 (NRR) and hydrolyzed reactive red 194 (HRR) forms from aqueous solutions. Chemical treatment of Brazilian pine-fruit shell (PW), with chromium (Cr–PW), with acid (A–PW), and with acid followed by chromium (Cr–A–PW) were also tested as alternative biosorbents for the removal of NRR and HRR from aqueous effluents. It was observed that the treatment of the Brazilian pine-fruit shell with chromium (Cr–PW and Cr–A–PW) led to a remarkable increase in the specific surface area and average porous volume of these biosorbents when compared to unmodified Brazilian pine-fruit shell (PW).

The effects of shaking time, biosorbent dosage and pH on biosorption capacity were studied. In acidic pH region (pH 2.0) the biosorption of NRR and HRR were favorable. The contact time required to obtain the equilibrium was 24 h at 25 °C.

The equilibrium data were fitted to Langmuir, Freundlich, Sips and Redlich–Peterson isotherm models. For NRR reactive dye the equilibrium data were best fitted to the Sips isotherm model using PW and A–PW as biosorbents, and Redlich–Peterson isotherm model using Cr–PW and Cr–A–PW as biosorbents. For HRR reactive dye the equilibrium data were best fitted to the Sips isotherm model using PW, A–PW and Cr–A–PW and the Redlich–Peterson isotherm model for Cr–PW as biosorbent.

© 2007 Elsevier B.V. All rights reserved.

Keywords: Biosorption; Brazilian pine-fruit shell; Modified biosorbent; Reactive red 194; Isotherms

1. Introduction

Reactive dyes are extensively used for coloring fabrics, because they present medium to high fastness to cellulose fibers [1]. High volumes of aqueous effluents contaminated with dyes are generated by textile industries. The removal of synthetic dyes from aquatic systems, is extremely important from the healthiness viewpoint [2,3] because most of these dyes are toxic, causing allergy, skin irritation, besides most of them are mutagenic and/or carcinogenic [2–4]. Therefore, industrial effluents

containing dyes need to be treated before being delivered to environment.

The most efficient procedure for removal of synthetic dyes from industrial effluents is the adsorption procedure, because the dye species are transferred from the water effluent to a solid phase, diminishing the effluent volume to a minimum. Subsequently, the adsorbent can be regenerated or kept in a dry place without direct contact with the environment.

Activated carbon is the most employed adsorbent for dye removal from aqueous solution because of its excellent adsorption properties [5–7]. However, the extensive use of activated carbon for dye removal from industrial effluents is expensive, limiting its large application for wastewater treatment. Therefore, there is a growing interest in finding alternative low cost adsorbents for dye removal from aqueous solution. Among these

* Corresponding author. Tel.: +55 51 3308 7175; fax: +55 51 3308 7304.
E-mail addresses: ederlima@iq.ufrgs.br, profederlima@gmail.com (E.C. Lima).

Nomenclature

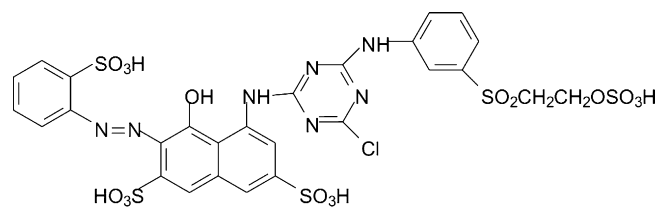
a_{RP}	the Redlich–Peterson constants (mg L^{-1}) ^{-β}
C	constant related with the thickness of boundary layer (mg g^{-1})
C_e	dye concentration at the equilibrium (mg L^{-1})
C_o	initial dye concentration put in contact with the adsorbent (mg L^{-1})
dq	differential of q
g	The Redlich–Peterson exponent (dimensionless)
h_o	the initial sorption rate ($\text{mg g}^{-1} \text{h}^{-1}$) of pseudo-second order equation
k_f	pseudo-first order rate constant (h^{-1})
k_{id}	intra-particle diffusion rate constant ($\text{mg g}^{-1} \text{h}^{-0.5}$)
k_s	the pseudo-second order rate constant ($\text{g mg}^{-1} \text{h}^{-1}$)
K_F	the Freundlich constant related with adsorption capacity ($\text{mg g}^{-1} (\text{mg L}^{-1})^{-1/n}$)
K_L	Langmuir affinity constant (L mg^{-1})
K_{RP}	Redlich–Peterson constants (L g^{-1})
K_S	the Sips constant related with affinity constant (mg L^{-1}) ^{-1/n}
m	mass of adsorbent (g)
n	dimensionless exponents of Freundlich and Sips equations
q	amount adsorbed of the dye by the adsorbent (mg g^{-1})
q_e	amount adsorbate adsorbed at the equilibrium (mg g^{-1})
q_t	amount of adsorbate adsorbed at time t (mg g^{-1})
Q_{\max}	the maximum adsorption capacity of the adsorbent (mg g^{-1})
t	time of contact (h)
V	volume of dye put in contact with the adsorbent (L)

Greek letters

α	the initial adsorption rate ($\text{mg g}^{-1} \text{h}^{-1}$) of Elovich equation
β	Elovich constant related to the extent of surface coverage and also to the activation energy involved in chemisorption (g mg^{-1})

alternative adsorbents, it can be cited: carbonized organic materials [8,9], fly-ashes [9,10], peat [9], moss [9], recycled alum sludge [11], earths [12,13], agricultural residues [4,9,14–18], fishery residues [9,19], microorganisms such as fungus [9], bacteria [9], and also algae [20].

In the present work it is proposed by the first time the use of Brazilian pine-fruit shell (*Araucaria angustifolia* syn. *Araucaria brasiliensis*), named piñon, in natural form or after some chemical treatment as a biosorbent for successful removal of C.I. Reactive Red 194 dye from aqueous solutions. This dye is largely used for textile dyeing in the Brazilian cloth industries and



Scheme 1. Structural formula of Reactive Red 194 ($\text{C}_{27}\text{H}_{22}\text{N}_7\text{O}_{16}\text{S}_5\text{Cl}$). MW 896.29 g mol^{-1} ; solubility 65 g L^{-1} ; λ_{\max} = 500 nm at pH 2.0. CI 18214, CAS registry number: 23354-52-1.

this work brings the first application of adsorption procedure to remove C.I. Reactive Red 194 from aqueous effluents.

2. Materials and methods

2.1. Solutions and reagents

De-ionized water was used throughout for solution preparations.

The textile reactive dye, C.I. Reactive Red 194 (see Scheme 1) assigned as NRR, was used in the biosorption experiments. It was obtained from Cotton Química (Novo Hamburgo-RS, Brazil), as a commercially available textile dye with a formulation designated as Rubi Reativo XLR-3, of 85% purity.

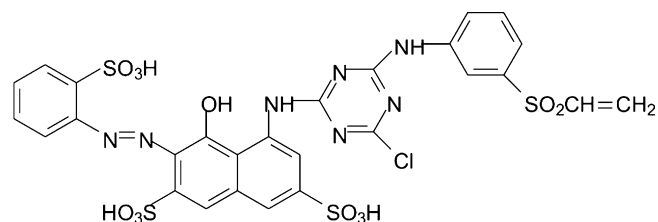
The stock solution was prepared by dissolving accurately weighted of dye in water, in order to obtain 1000 mg L^{-1} of NRR.

To simulate dye-bath effluents from dyeing processes, hydrolysis of dye was accomplished by refluxing 588 mg (85% purity) of NRR dye with 0.1 mol L^{-1} NaOH, as reported elsewhere [1]. After that, the volume was completed to 500 mL, obtaining a stock solution with concentration of 1000 mg L^{-1} of hydrolyzed dye, which was assigned as HRR (see Scheme 2).

The working solutions of NRR and HRR were obtained by diluting the dye stock solutions to the required concentrations. The pH adjustments of the solutions were made with aliquots of 1.0 mol L^{-1} of HCl and NaOH.

2.2. Adsorbents preparation and characterization

Brazilian pine-fruit (piñon) was acquired at local market in Porto Alegre-RS, Brazil. The weight of each seed varied between 7 and 9 g. The seed shells correspond to approximately 22% of the whole Brazilian pine-fruit. About 2 kg of Brazilian pine-fruit was cooked in a 10 L glass beaker for 2 h, and then the seeds were separated from the shells. The brown aqueous solution



Scheme 2. Structural formula of hydrolyzed Reactive Red ($\text{C}_{27}\text{H}_{20}\text{N}_7\text{O}_{12}\text{S}_4\text{Cl}$) assigned as HRR. MW 798.21 g mol^{-1} ; λ_{\max} = 515 nm at pH 2.0.

which resulted from the Brazilian pine-fruit cooking containing oxidized phenols [21,22] was discarded. Subsequently, the Brazilian pine-fruit shell were immersed in 2 L of de-ionized water and it was again heated to boil for two more hours, in order to remove the water soluble phenolic compounds [21,22], and to avoid releases of these compounds to the water solutions, during the biosorption experiments. Subsequently, the Brazilian pine-fruit shell was washed with distilled water, dried at 70 °C in an air-supplied oven for 8 h. After that, the Brazilian pine-fruit shell was grounded in a disk-mill and subsequently sieved. The part of biosorbent with diameter of particles $\leq 250 \mu\text{m}$ was used. This unmodified Brazilian pine-fruit shell was assigned as PW.

In order to evaluate the reutilization of PW loaded with chromium, as previously reported [21], as biosorbent for removal of NRR and HRR from aqueous effluents, PW were subject to some chemical treatments as described below.

An amount of 5.0 g of PW was added to 200.0 mL of 500 mg L⁻¹ of Cr(VI) solution (pH 2.0), and the slurry was magnetically stirred for 24 h. Subsequently, the slurry was filtrated in a sintered glass funnel, and the solid phase was thoroughly washed with water, until the filtrate reached the pH of distilled water. Subsequently, the material was dried at 70 °C in an air-supplied oven for 8 h, yielding chromium adsorbed on Brazilian pine-fruit shell assigned as Cr–PW [21]. Similar procedure was carried out using 5.0 g of PW and 0.5 mol L⁻¹ of HCl obtaining acid treated Brazilian pine-fruit shell assigned as A–PW; and additionally 2.0 g of A–PW was treated with 500 mg L⁻¹ of Cr(VI) solution in a similar procedure, obtaining chromium adsorbed on acid treated Brazilian pine-fruit shell, which was assigned as Cr–A–PW [21].

The biosorbents PW, Cr–PW, A–PW and Cr–A–PW were characterized by FTIR using a Shimadzu FTIR, model 8300 (Kyoto, Japan). The spectra were obtained with a resolution of 4 cm⁻¹, with 100 cumulative scans.

The PW biosorbent sample was submitted to thermal gravimetric analysis (TGA), using argon atmosphere. The equipment used was a Shimadzu model TGA-502. The samples were heated from room temperature to 800 °C at a rate of 20 °C min⁻¹.

The N₂ adsorption/desorption isotherms of the biosorbents were obtained at liquid nitrogen boiling point, in a homemade volumetric apparatus, with a vacuum line system employing a turbo molecular Edwards vacuum pump. The pressure measurements were made using capillary Hg barometer. The apparatus was frequently checked with an alumina (Aldrich) standard reference (150 mesh, 5.8 nm and 155 m² g⁻¹). Prior to the measurements, the biosorbent samples were degassed at 150 °C, in vacuum, for 2 h. The specific surface areas were determined from the Brunauer, Emmett and Teller (BET) [23] multipoint method and the pore size distribution were obtained using Barret, Joyner, and Halenda (BJH) method [24].

The biosorbents samples were also analyzed by scanning electron microscopy (SEM) in Jeol microscope, model JEOL JSM 6060, using an acceleration voltage of 20 kV and magnification ranging from 100 to 40,000-fold.

For determination of major mineral components of the PW biosorbent, a digestion procedure using nitric acid and hydrogen peroxide, as described elsewhere [25], was employed. The

Table 1
Physical and chemical properties of the biosorbents

Specific surface area—BET (m ² g ⁻¹)	
PW	63 ± 8
Cr–PW	300 ± 20
A–PW	153 ± 10
Cr–A–PW	215 ± 15
Average pore volume (cm ³ g ⁻¹)	
PW	0.07 ± 0.01
Cr–PW	0.13 ± 0.01
A–PW	0.08 ± 0.01
Cr–A–PW	0.12 ± 0.01
Zero charge potential (pH)	
PW	4.73
Cr–PW	4.20
A–PW	3.41
Cr–A–PW	3.79
Elemental analysis for PW	
C (%)	44.21
H (%)	13.17
N (%)	0.41
Carbonyl groups for PW (mmol g ⁻¹)	0.01
Phenolic (mmol g ⁻¹)	1.86
Ashes content (%)	1.76
Total fiber (%)	32.3
Mineral composition of PW	
Na (%)	0.102
K (%)	0.0980
Ca (%)	0.214
Mg (%)	0.114
P (%)	0.203
Fe (%)	0.062
Al (%)	0.101
Mn (%)	0.0450
Zn (%)	0.0034
Cu (%)	0.0012

mineral composition of the PW biosorbent present in the digest of the biomaterial was determined by flame atomic absorption spectrometry using an Analyst 200 spectrometer (PerkinElmer).

The elemental analysis of the PW biosorbent was carried out on a CHN PerkinElmer M CHNS/O Analyzer, Model 2400, after degassing treatment at 150 °C. The analyses were made in triplicate.

The total fiber contents of PW biosorbent was evaluated as described elsewhere [26].

The zero charge potentials of the four biosorbents were measured by the mass titration [27] methods.

The physical and chemical properties of the biosorbents are presented in Table 1.

2.3. Biosorption studies

The biosorption studies for evaluation of the biosorbents (PW, Cr–PW, A–PW and Cr–A–PW) for removal of the dyes (NRR and HRR) from aqueous solutions were carried-out in triplicate using the batch biosorption procedure. For these experiments, fixed amount of biosorbents (20.0–500.0 mg) were placed in a 50 mL glass Erlenmeyer flasks containing 20.0 mL of dye solutions (2.00–500.0 mg L⁻¹), which were agitated for a suitable

time (0.08–72 h) at 25 °C. The pH of the dye solutions ranged from 2.0 to 10.0. Subsequently, in order to separate the biosorbents from the aqueous solutions, the flasks were centrifuged at 2400 rpm for 10 min, and aliquots of 1–10 mL the supernatant were properly diluted with water.

The final concentrations of the dye remained in the solution were determined by visible spectrophotometry, using a Femto spectrophotometer provided with optical-glass cells. Absorbance measurements were made at the maximum wavelength of NRR and HRR which were 500 and 515 nm, respectively, at pH 2.0.

Batch desorption studies were carried out by agitating 20.0 mL of dye solution of 25.0 mg L⁻¹ and 50.0 mg of biosorbent, the agitation time used was 48 h, and the supernatant dye solution was discarded. The amount of the dye adsorbed on the biosorbents, were firstly washed with water for removing non-adsorbed dye. Then, the dye adsorbed on the biosorbent was agitated with 20.0 mL of aqueous solutions (0.050–0.15 mol L⁻¹ NaOH or 0.050–0.50 mol L⁻¹ NaCl or KCl) up to 1 h. The desorbed dye was separated and estimated as described above.

Amount of the dyes uptaken by the biosorbents were calculated by applying the equation:

$$q = \frac{C_o - C_e}{m} V \quad (1)$$

2.4. Statistical evaluation of the kinetic and isotherm parameters

In this work, the kinetic and equilibrium models were fitted employing the non-linear fitting method using the non-linear fitting facilities of the software Microcal Origin 7.0. In addition, the models were also evaluated by probability plot of the residuals (difference between the $q_{i \text{ model}}$ and $q_{i \text{ experimental}}$), where $q_{i \text{ model}}$ is each value of q predicted by the fitted model and $q_{i \text{ experimental}}$ is each value of q measured experimentally [28], by using the Minitab Statistical Software release 14.20.

3. Results and discussion

3.1. Characterization of biosorbents

The physical and chemical properties of PW, Cr-PW, A-PW and Cr-A-PW are presented in Table 1. The pore size distributions of the four biosorbents, obtained by BJH method, are shown in Fig. 1. As can be seen, the distribution of average pore diameter curve present two maxima, the highest peak ranging from 0.95 to 0.98 nm and the second peak ranging from 3.6 to 4.1 nm. These curves indicate that the diameter pore region of the first peak is present in higher amount when compared with the second peak. Therefore, these adsorbents can be considered mixtures of microporous and mesoporous materials [23,24,28], containing predominantly microporous, which is defined as a material that presents average diameter pore lower than 2 nm [23,24,28]. Also there are lower fractions with mesopores with diameters ranging from 3.6 to 12 nm [23,24,28].

It was also observed that the chemical treatments of the piñon fiber with chromium promoted remarkable changes in the morphology of the fiber. The specific surface areas increased up to four to five times, and the pore volumes were practically doubled (see Table 1) when Cr-PW and Cr-A-PW were compared to PW alone.

Fig. 2A shows the FTIR vibrational spectrum of Brazilian pine-fruit shell (PW). The absorption bands at 3357 and 2900 cm⁻¹ are assigned to O–H bonds (stretch) of macromolecular association, and C–H bonds (stretch), respectively [29,30]. The sharp intense peak observed at 1609 cm⁻¹ is assigned to C=C ring stretch of aromatic rings [29]. In addition the bands of 1510 and 1425 cm⁻¹ confirm the presence of C=C of aromatic rings [30]. Several bands ranging from 1319 to 1030 cm⁻¹ refer to C–O bonding of phenols [29]. This splitting pattern is characteristic of several different C–O bonding of different phenols, indicating that Brazilian pine-fruit shell is rich on tannins, as already reported [21,22]. These FTIR results are corrobo-

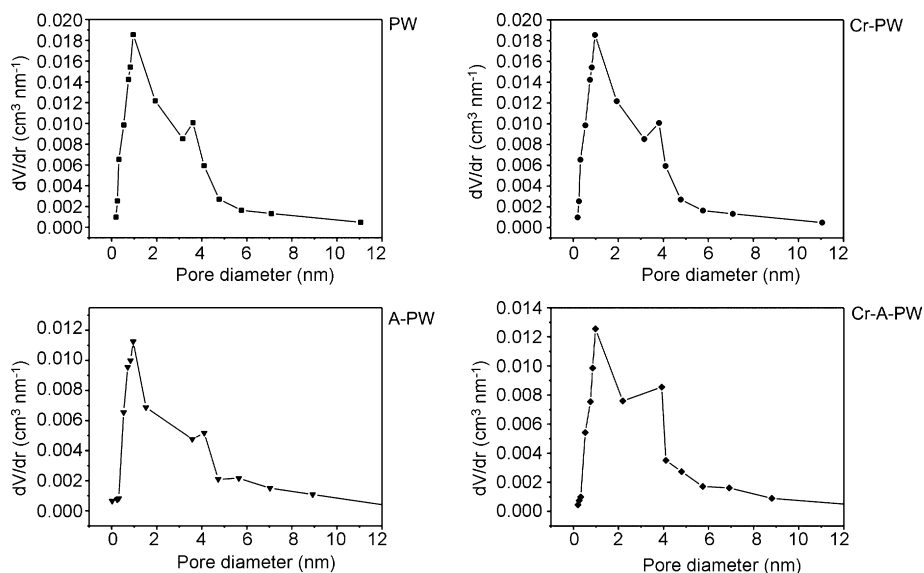


Fig. 1. Pore size distribution of biosorbents obtained by BJH method.

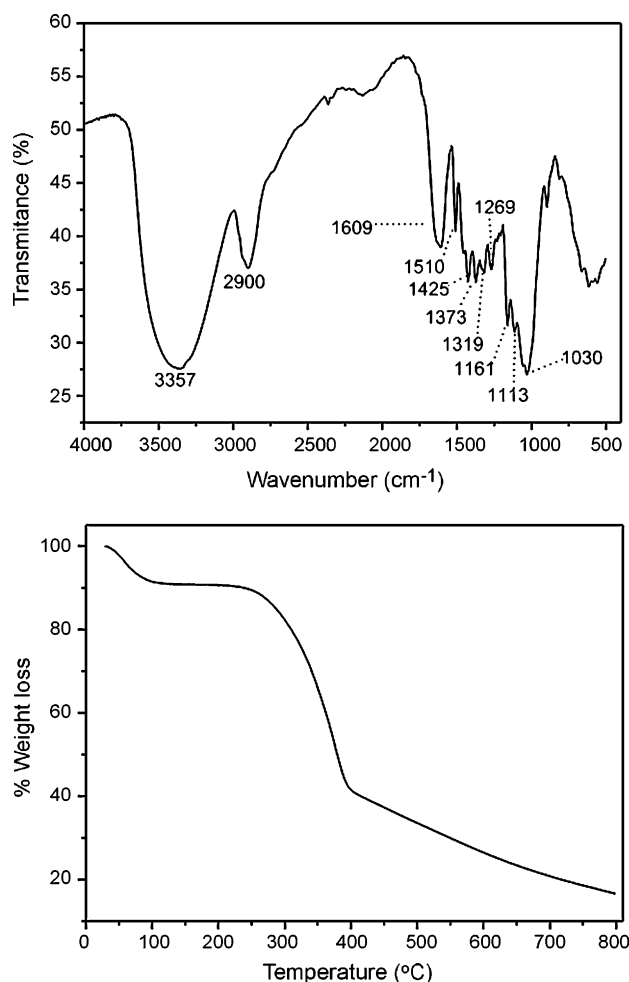


Fig. 2. (A) FTIR spectrum of PW biosorbent and (B) TGA curve for PW biosorbent in argon atmosphere.

rated by the amount of phenolic groups on the material and with the elemental analysis (see Table 1) indicating that the PW presents functional groups such as, OH, aromatic rings that can be potential biosorption sites for interaction with the sulfonic groups of the dyes. The FTIR spectra for the A-PW, Cr-PW and Cr-A-PW, did not present any relevant changes in relation to PW, therefore they were not shown.

The PW biosorbent was submitted to thermal gravimetric analysis under argon atmosphere, the TGA curve is presented in Fig. 2B. The weight loss (10%) from room temperature up to 150 °C was due to water desorption. From 150 to 240 °C the material was very thermally stable. This high thermal stability is an exceptional characteristic for fibrous biosorbents, allowing analyzing its structure by N₂ adsorption/desorption isotherm curves. Besides that, swelling tests of PW biosorbent were also performed, and the increase in the volume was lower than 4%, confirming the rigidity of the Brazilian pine-fruit shell.

Scanning electron microscopies (SEM) of the four different biosorbents employed in this work are shown in Fig. 3. These micrographs show the fibrous structure of PW, Cr-PW, A-PW and Cr-A-PW. Some fissures and holes in these fibers can be seen, which indicate the presence of small number of macroporous structure, that could contribute a little bit to the biosorption

of the dyes (NRR and HRR), however the best contribution of the dyes biosorption can be attributed to micro- and meso-porous structures (see Fig. 1) which can not be visualized in the scanning electron microscopies.

3.2. Acidity effects on the biosorption of dyes

Fig. 4 shows the dependence of NRR dye removal for various pH solutions using the four biosorbents employed. The amount of dye uptake decreases abruptly with increases in the pH solutions ranging from 2.5 up to 6.0 for all cases. For pH values higher than 4.5, practically no dye was adsorbed. The maximum biosorptions of the NRR occurred at pH values ranging from 1.5 to 2.0. For HRR dye, similar behavior was also observed for the four biosorbents. In this sense, all the further experiments were carried out at a solution pH of 2, to avoid disruption of the fiber structure of the biosorbents, as reported elsewhere [21].

The higher amount of NRR and HRR adsorbed by the four biosorbents (PW, Cr-PW, A-PW and Cr-A-PW) at lower pH values can be explained, considering the electrostatic interactions between the surface charge of the biosorbents, which became positively charged at $\text{pH} \leq 2.0$ ($\text{pH} < \text{pH}_{\text{ZPC}}$), with the negatively charged dyes. It should be highlighted that sulfonic groups present negative charge even at higher acidic solutions, because their pK_a values are lower than zero [31]. In addition, at pH 2.0, the biosorbents present positive surface charge, since all the zero charge potentials of these biosorbents are lower than 4.73 ($\text{pH} < \text{pH}_{\text{ZPC}}$) (see Table 1).

3.3. Effects of adsorbent dosage

The study of biosorbent dosage of PW, Cr-PW, A-PW and Cr-A-PW for removal of the NRR and HRR dyes from aqueous solution was carried-out at different biosorbent doses (1.0–25.0 g L⁻¹) using a 25.0 mg L⁻¹ of dyes. It was observed that quantitative removal of the dyes was attained for biosorbent dosage of at least 5.0 g L⁻¹. For biosorbent dosage higher than this value, the dye removal remained almost constant. Increase in the percentage of dye removal with adsorbent dosage could be attributed to increase in the adsorbent surface areas, augmenting the number of biosorption sites available for biosorption, as already reported [32]. Therefore, in the further experiments, the adsorbent dosage was fixed to 5.0 g L⁻¹.

3.4. Biosorption kinetics and desorption experiments

Adsorption kinetic study is important in treatment of aqueous effluents as it provides valuable information on the reaction pathways and in the mechanism of adsorption reactions [33–37]. In Table 2 are summarized some of the most important kinetic models, which were employed in this work, for describing the biosorption of NRR and HRR reactive dyes on the PW, Cr-PW, A-PW and Cr-A-PW biosorbents. The fitting of these kinetic models are presented in Fig. 5. The kinetic parameters of the fitted models are presented in Table 3. As can be seen, the pseudo second-order, and the Elovich chemisorption models are suitably fitted, presenting good residual analysis [28], with low standard

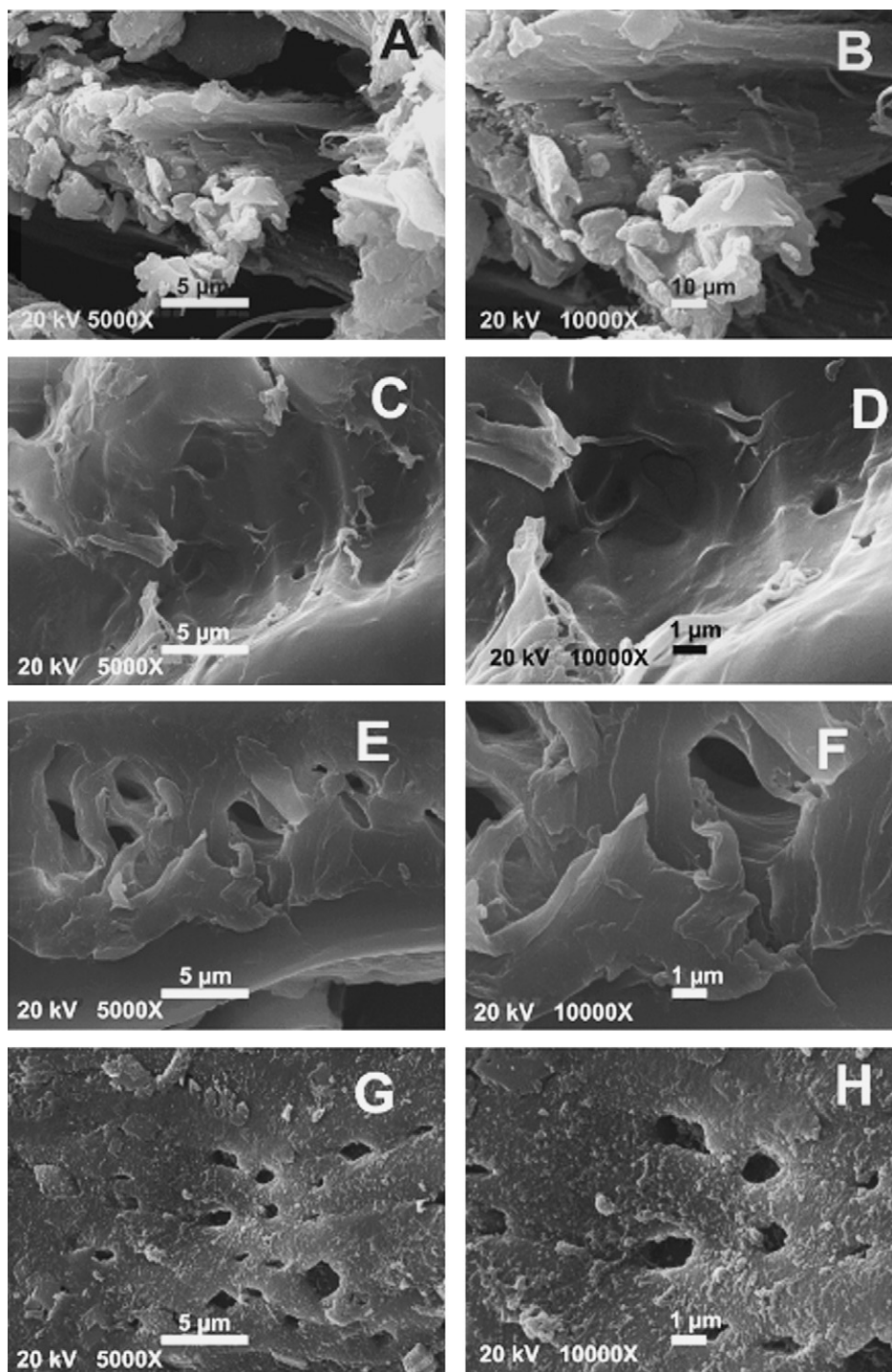


Fig. 3. Scanning electron microscopy for (A) PW, 5,000 \times ; (B) PW, 10,000 \times ; (C) Cr-PW, 5,000 \times ; (D) Cr-PW, 10,000 \times ; (E) A-PW, 5,000 \times ; (F) A-PW, 10,000 \times ; (G) Cr-A-PW, 5,000 \times ; (H) Cr-A-PW, 10,000 \times .

deviations of the residuals and averages of the residues close to zero, besides of presenting probabilities higher than 0.05, that indicate the absence of systematic deviations of the q values obtained by the model ($q_{i \text{ model}}$) from the q values measured experimentally ($q_{i \text{ experimental}}$). The residual analysis is a probability plot of residuals ($q_{i \text{ model}} - q_{i \text{ experimental}}$) placed at the abscissa versus probability placed at coordinate. Each point is an individual residual. If the residual follow a normal distribu-

tion pattern, the point will be placed close to the central line that presents zero of residual at probability of 0.5. How small the distribution of the residual at the abscissa, small is the standard deviation of the residual, meaning that the q values obtained by the proposed model agree with the experimental values of q . In addition, if the residual follow a normal distribution, half of the residual will be distributed at abscissa with values lower than zero (negative) and half of the residual will be distributed at

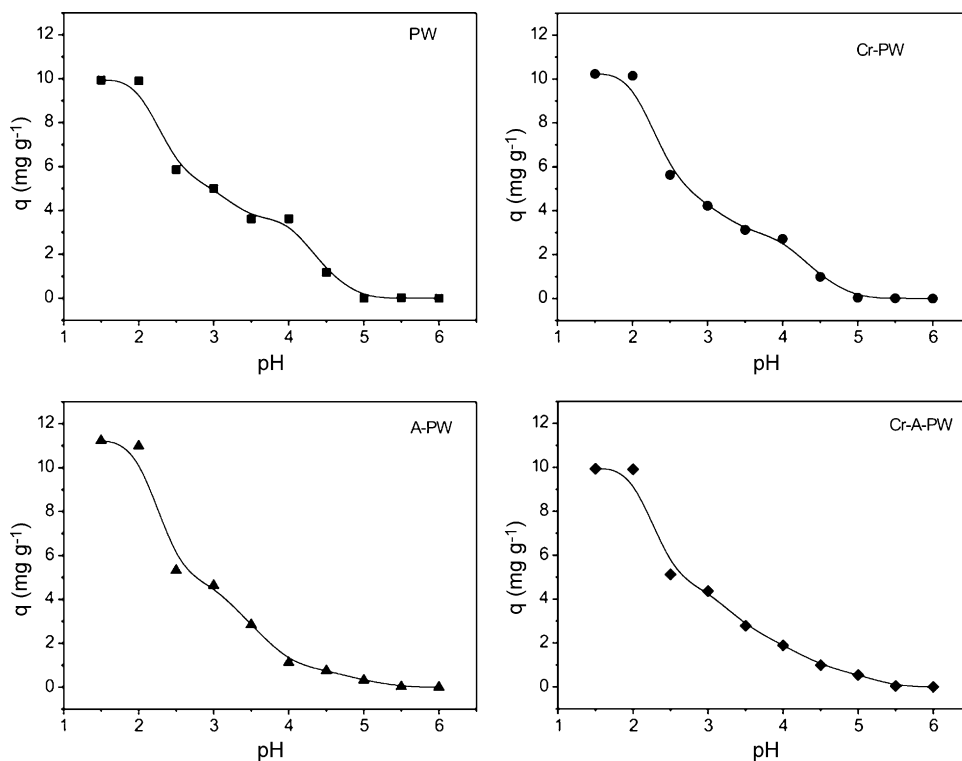


Fig. 4. Effects of pH on the removal of NRR from aqueous solution, using an initial concentration of 30.0 mg L^{-1} , and the temperature was fixed at 25°C .

abscissa with values higher than zero (positive). If the residuals are within the confidence interval at 95% of confidence level, each individual residual could not be placed outside the confidence band. If it occurs its probability is lower than 5% (<0.05). For simplicity reasons, only two of a total of thirty and two probability plots dealing with the kinetics fitting are shown in Fig. 6.

From all these four kinetic models, the pseudo second-order kinetic model is a little bit better fitted when compared with the Elovich chemisorption model, since it presented lower standard deviation of the residues ($<0.202 \text{ mg g}^{-1}$), which means that the q fitted by this model was closer to q experimentally measured for the all the experimental points. The residual analysis are also confirmed by the value of R^2 , however the normal distribution of the residuals gives a better idea about the fitting of each individual point, as early discussed [28]. Therefore the pseudo second-order, and Elovich chemisorption models in decreasing order, should explain the biosorption of the dyes (NRR and HRR) by using the four biosorbents (PW, Cr-PW, A-PW and Cr-A-PW). In addition, it was verified that the models intra-

particle diffusion and pseudo-first order kinetic models were not suitably fitted in several cases, presenting probability of the residuals ($q_{i \text{ model}} - q_{i \text{ experimental}}$) lower than 0.05, which means that the residuals does not follow normal distributions at 95% of confidence level, indicating that these models presented some systematic deviations of the q fitted by the model from the q measured in the experiments.

Based on these kinetic results and on the previously described results, there are several arguments to state that the biosorption mechanism of NRR and HRR dyes on PW, Cr-PW, A-PW and Cr-A-PW biosorbents should follow an electrostatic mechanism, *i.e.*, the positively surface charged biosorbents at pH values of 2.0 (see Table 1—zero charge potentials for all biosorbents), should attract the negatively charged sulfonic groups [31] present in the dyes.

In order to confirm the electrostatic attraction of the positively surface charged biosorbent at pH 2.0 with the negative charged dye, desorption experiments were carried-out. Several solutions containing $0.05\text{--}0.15 \text{ mol L}^{-1}$ of NaOH and $0.05\text{--}0.50 \text{ mol L}^{-1}$ of KCl or NaCl were tested for regeneration of the loaded biosor-

Table 2
Kinetic adsorption models

Kinetic model	Differential equation	Integrated equation	Non-linear equation	Ref.
Pseudo-first order	$\frac{dq}{dt} = k_f(q_e - q_t)$	$\ln(q_e - q_t) = \ln(q_e) - k_f t$	$q_t = q_e[1 - \exp(-k_f t)]$	[33]
Pseudo second order	$\frac{dq_t}{dt} = k_s(q_e - q_t)^2$	$q_t = \frac{k_s q_e^2 t}{1 + q_e k_s t}$	$q_t = \frac{k_s q_e^2 t}{1 + q_e k_s t}$, $h_0 = k_s q_e^2$, initial sorption rate	[34]
Elovich	$\frac{dq}{dt} = \alpha \exp(-\beta q_t)$	$q_t = \frac{1}{\beta} \ln(t + t_0) - \frac{1}{\beta} \ln(t_0)$	$q_t = \frac{1}{\beta} \ln(\alpha\beta) + \frac{1}{\beta} \ln(t)$	[15]
Intra-particle diffusion			$q_t = k_{id} \sqrt{t} + C$	[35]

Table 3
Kinetic parameters and residual analysis for NRR and HRR biosorption, using PW, Cr–PW, A–PW and Cr–A–PW as biosorbents

	NRR				HRR			
	PW	Cr–PW	A–PW	Cr–A–PW	PW	Cr–PW	A–PW	Cr–A–PW
Pseudo-first order								
k_f (h^{-1})	0.153 ± 0.002	0.283 ± 0.096	0.239 ± 0.01	0.137 ± 0.009	0.153 ± 0.01	0.232 ± 0.01	0.244 ± 0.08	0.130 ± 0.1
q_c (mg g^{-1})	6.89 ± 0.1	6.14 ± 0.28	7.25 ± 0.1	7.72 ± 0.1	7.21 ± 0.1	6.01 ± 0.08	6.38 ± 0.01	7.74 ± 0.008
R^2	0.9469	0.9440	0.9244	0.9685	0.9570	0.9721	0.9681	0.9721
Residual analysis								
Average of residuals	-7.04×10^{-2}	-3.05×10^{-2}	4.45×10^{-2}	-6.50×10^{-2}	-5.69×10^{-2}	-2.59×10^{-2}	-3.02×10^{-2}	-6.58×10^{-2}
Standard deviation	0.401	0.300	0.447	0.361	0.388	0.230	0.253	0.341
Probability	0.260	0.095	0.199	0.176	0.332	0.021	0.026	0.153
Pseudo-second order								
k_s ($\text{g mg}^{-1} \text{h}^{-1}$)	$2.17 \times 10^{-2} \pm 1 \times 10^{-3}$	$5.73 \times 10^{-2} \pm 2 \times 10^{-3}$	$3.78 \times 10^{-2} \pm 2 \times 10^{-3}$	$1.65 \times 10^{-2} \pm 9 \times 10^{-4}$	$2.03 \times 10^{-2} \pm 0.001$	$4.41 \times 10^{-2} \pm 1 \times 10^{-3}$	$4.51 \times 10^{-2} \pm 9 \times 10^{-4}$	$1.54 \times 10^{-2} \pm 8 \times 10^{-4}$
q_c (mg g^{-1})	8.17 ± 0.1	6.84 ± 0.05	8.22 ± 0.01	9.27 ± 0.1	8.59 ± 0.1	6.82 ± 0.04	7.20 ± 0.03	9.35 ± 0.1
h_o ($\text{mg g}^{-1} \text{h}^{-1}$)	1.45	2.68	2.55	1.42	1.50	2.05	2.34	1.35
R^2	0.9867	0.9935	0.9866	0.9937	0.9916	0.9965	0.9987	0.9941
Residual analysis								
Average of residuals	-2.57×10^{-2}	-4.68×10^{-3}	-9.37×10^{-3}	-1.89×10^{-2}	-1.68×10^{-2}	-7.55×10^{-4}	-2.68×10^{-3}	-2.08×10^{-2}
Standard deviation	0.202	0.103	0.189	0.163	0.173	0.0824	0.0512	0.158
Probability	0.880	0.677	0.748	0.227	0.242	0.443	0.838	0.224
Elovich chemisorption								
α ($\text{mg g}^{-1} \text{h}^{-1}$)	3.74 ± 0.21	9.98 ± 0.2	7.70 ± 0.5	3.48 ± 0.1	3.70 ± 0.1	5.94 ± 0.6	7.26 ± 0.4	3.30 ± 0.2
β (g mg^{-1})	0.618 ± 0.01	0.866 ± 0.03	0.668 ± 0.01	0.529 ± 0.01	0.577 ± 0.01	0.796 ± 0.03	0.774 ± 0.03	0.524 ± 0.01
R^2	0.9917	0.9713	0.9913	0.9897	0.9936	0.9695	0.9715	0.9891
Residual analysis								
Average of residuals	-5.26×10^{-11}	2.92×10^{-18}	1.32×10^{-10}	1.14×10^{-10}	5.26×10^{-11}	2.10×10^{-10}	1.05×10^{-10}	5.26×10^{-11}
Standard deviation	0.1608	0.216	0.153	0.209	0.151	0.242	0.241	0.218
Probability	0.864	0.119	0.061	0.188	0.917	0.157	0.088	0.717
Intra-particle diffusion								
Kid ($\text{mg g}^{-1} \text{h}^{-0.5}$)	0.973 ± 0.06	0.663 ± 0.07	0.876 ± 0.07	1.13 ± 0.07	1.04 ± 0.07	0.719 ± 0.07	0.740 ± 0.08	1.15 ± 0.07
C (mg g^{-1})	1.58 ± 0.2	2.77 ± 0.3	2.75 ± 0.3	1.43 ± 0.3	1.57 ± 0.2	2.26 ± 0.3	2.55 ± 0.2	1.31 ± 0.3
R^2	0.9401	0.8372	0.8890	0.9321	0.9315	0.8326	0.8336	0.9362
Residual analysis								
Average of residuals	1.05×10^{-10}	5.26×10^{-11}	-5.26×10^{-11}	4.21×10^{-10}	-2.11×10^{-10}	1.58×10^{-10}	-5.26×10^{-11}	-5.26×10^{-11}
Standard deviation	0.4326	0.514	0.545	0.538	0.495	0.568	0.582	0.527
Probability	0.065	0.007	0.004	0.041	0.088	0.034	0.018	0.070

Conditions: temperature was fixed at 25 °C, pH 2.0, adsorbent dosage 5.0 g L⁻¹ and adsorbate concentration 25.0 mg L⁻¹.

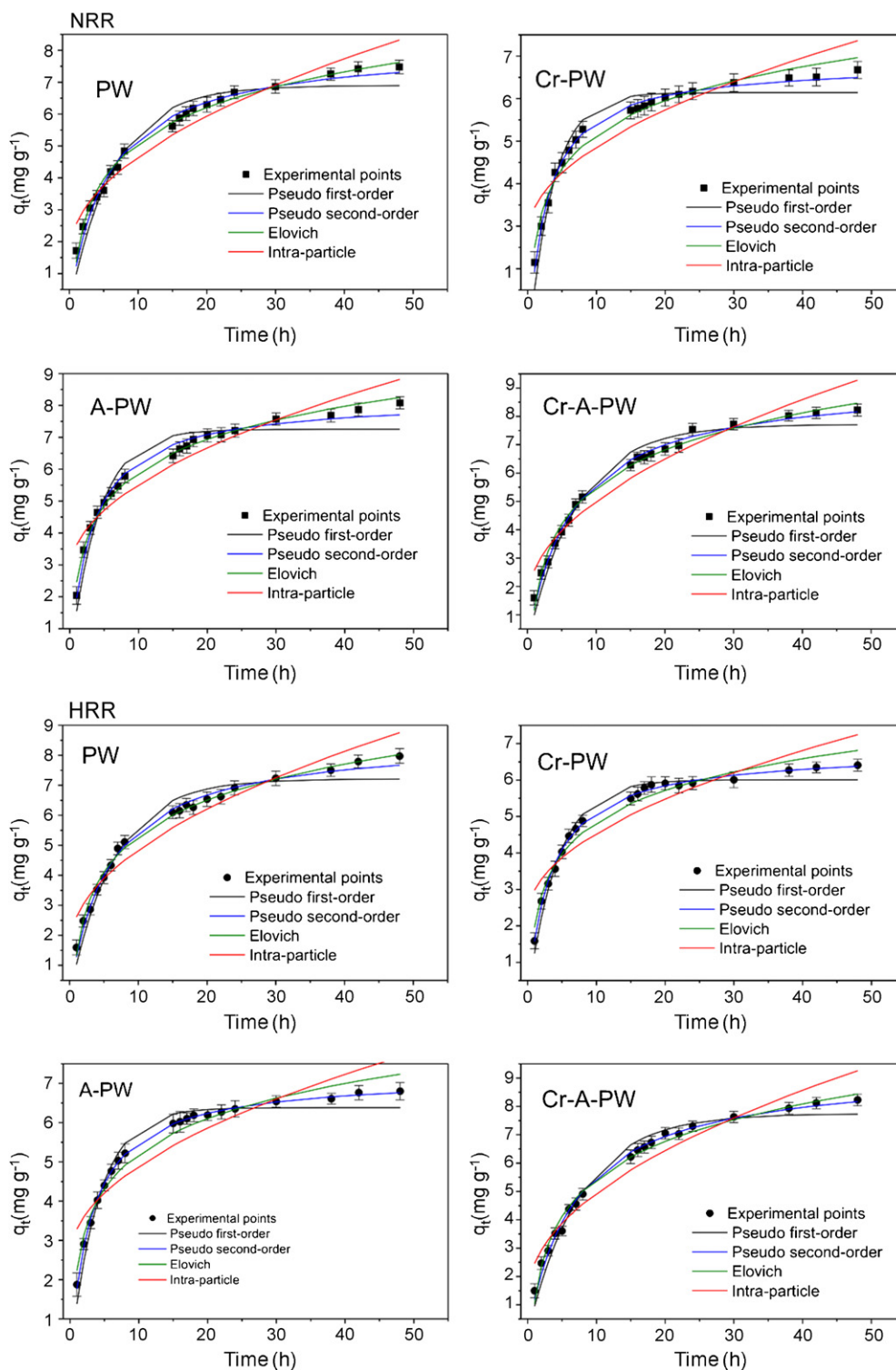


Fig. 5. Kinetic models for the removal of NRR and HRR from aqueous solution. Conditions: initial dye concentration of 25.0 mg L^{-1} , temperature was fixed at 25°C , pH 2.0, and biosorbent dosage of 5.0 g L^{-1} .

bent (see Fig. 7). It should be mentioned that the addition of solutions with concentrations higher than 0.05 mol L^{-1} NaOH desorbed the dye uptaken by the biosorbent immediately, on the other hand, the quantitative recoveries of the biosorbent using KCl and NaCl as regenerating solutions took about 1 h of agitation.

Based on all the results discussed therein, a proposed mechanism for NRR and HRR removal from aqueous solution is depicted on Scheme 3.

First of all, for initiating the biosorption process, the pH of the solution should be adjusted to values of 2.0, in order to protonated the phenolic groups present on the biosorbent surface

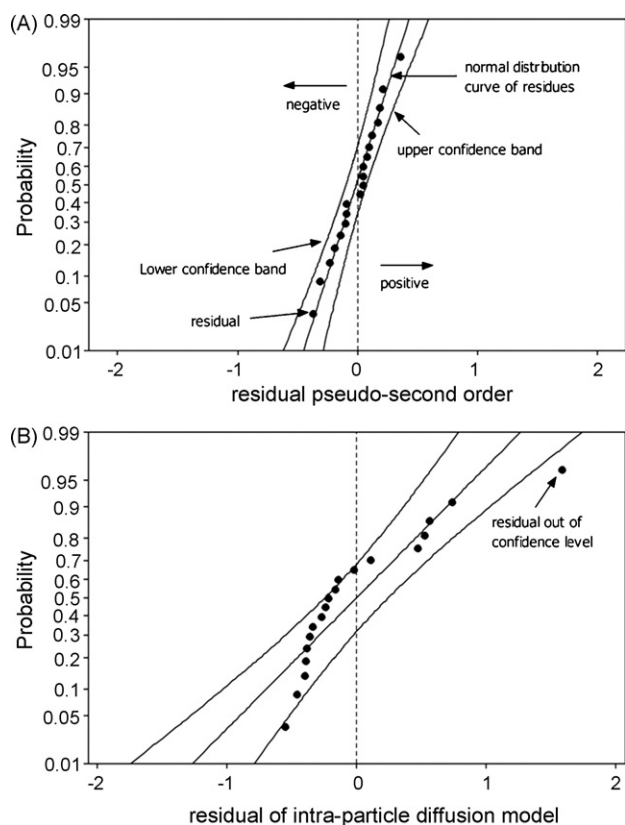


Fig. 6. Normal probability plot of residuals: (A) pseudo-second order; (B) intra-particle diffusion. Biosorbent A–PW, adsorbate NRR.

[21,22]. The second step depicted in the biosorption mechanism, is the electrostatic attraction of the negatively charged dye (sulfonic groups) with the positively surface charged biosorbent ($\text{pH} \leq 2.0$). The complete regeneration of the loaded biosorbent takes place using 0.50 mol L^{-1} of NaCl ($\text{pH} 7.0$) after about 1.0 h of contact time or with 0.10 mol L^{-1} of NaOH almost immediately (step 3).

It should be stressed that HCl employed for desorbing the dyes (NRR and HRR) of the biosorbents was not effec-

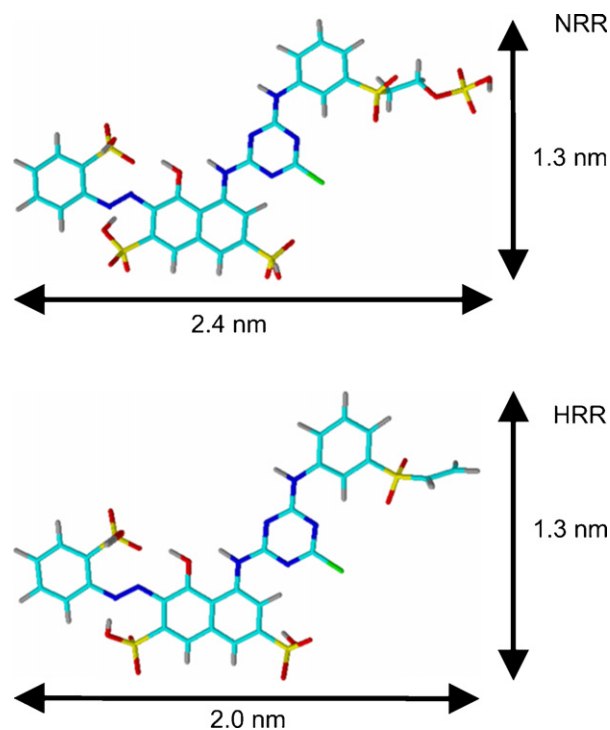


Fig. 8. Optimized three-dimensional structural formulae of NRR and HRR. The dimensions of the chemical molecule were calculated using ACD/LABS freeware version.

tive (see Fig. 7), corroborating the proposed mechanism of biosorption.

The contact time to reach the equilibration is long (about 24 h, see Fig. 5), since in the biosorbent materials, the presence of micropore structures were predominant in relation to mesoporous (see Fig. 1) and also to macroporous (see Fig. 3). The distribution curve of the pores size of PW, Cr–PW, A–PW and Cr–A–PW presented a maximum at 0.95, 0.97, 0.96 and 0.98 nm (see Fig. 1), respectively. Taking into account the molecular dimensions of NRR and HRR (see Fig. 8), calculated using the facilities of the software ACD/Labs version 10.0, the diffusion of

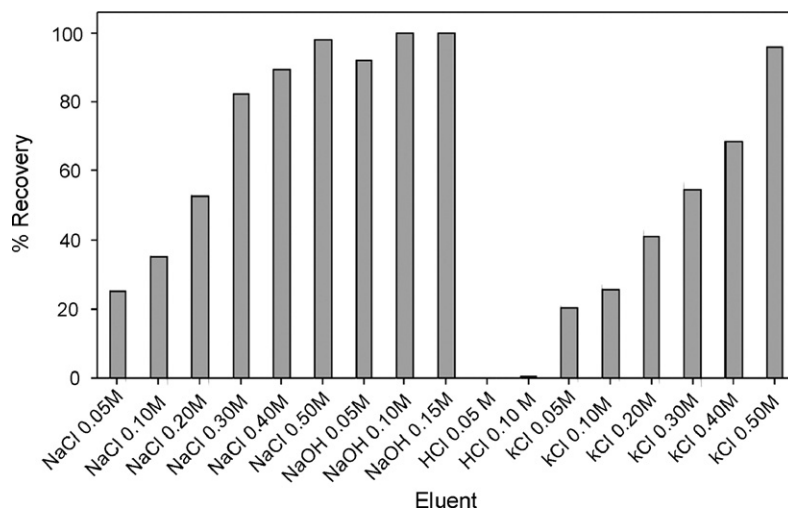


Fig. 7. Desorption of loaded A–PW biosorbent. Desorption experiments were carried out at 25°C during 1 h.

Table 4
Isotherm models

Isotherm model	Equation	Ref.
Langmuir	$q_e = \frac{Q_{\max} K_L C_e}{1 + K_L C_e}$	[39]
Freundlich	$q_e = K_F C_e^{1/n}$	[40]
Sips	$q_e = \frac{Q_{\max} K_S C_e^{1/n}}{1 + K_S C_e^{1/n}}$	[41]
Redlich–Peterson	$q_e = \frac{K_{RP} C_e}{1 + a_{RP} C_e^g}$ where $g \leq 1$	[42]

fast is the kinetic for establishment of the equilibrium involving the adsorbate and adsorbent. Based on this information, the bulk NRR and HRR dyes should present a slow kinetics of adsorption on the four biosorbents.

3.5. Equilibrium adsorption studies

In this work, the Langmuir [39], Freundlich [40], Sips [41] and Redlich–Peterson [42] isotherm models were tested and their equations are presented in Table 4.

The isotherms of biosorption of NRR and HRR dyes on PW, Cr–PW, A–PW and Cr–A–PW biosorbents were performed, using the best experimental conditions, which were: pH 2.0, contact time of 24 h, biosorbent dosage of 5.0 g L⁻¹, and temperature fixed at 25 °C (see Fig. 9). The data of the fitted models are presented in Table 5. Based on the residual analysis, the equilibrium data fit very well all the isotherm models for both adsorbents, with the exception of Freundlich model, which presents a maximum standard deviation of 4.29 mg g⁻¹, on the other hand the maximum standard deviation observed for all three models are up to 1.14 mg g⁻¹. It was observed that slightly better isotherm fitting, based on the residual analysis [28], were the Sips and Redlich–Peterson isotherm models, however the Langmuir model should also be taken into account, since it was properly fitted, presenting an average of the residuals close to zero, and a small standard deviation and a probability higher than 0.05.

In addition, it should be highlighted that the residual analysis is very important to interpret the isotherm fittings. When the residual distributions follow the normal pattern, it can be inferred that the model does not present any systematic deviation [28]. Additionally, it was also observed that the Sips

Table 5
Isotherm parameters for NRR and HRR biosorption, using PW, Cr–PW, A–PW and Cr–A–PW as biosorbents

	NRR				HRR			
	PW	Cr–PW	A–PW	Cr–A–PW	PW	Cr–PW	A–PW	Cr–A–PW
Langmuir								
Q_{\max} (mg g ⁻¹)	13.4 ± 0.3	20.7 ± 0.9	51.9 ± 0.3	41.6 ± 0.4	20.8 ± 0.4	29.3 ± 0.3	76.5 ± 0.8	61.1 ± 0.5
K_L (L mg ⁻¹)	0.184 ± 0.02	0.155 ± 0.03	0.124 ± 0.004	0.308 ± 0.02	0.0703 ± 0.07	0.0726 ± 0.002	0.0464 ± 0.001	0.0904 ± 0.003
R^2	0.9876	0.9710	0.9987	0.9919	0.9946	0.9980	0.9978	0.9982
Average of residuals	0.0394	-0.0321	-0.0468	0.0459	-0.0995	-3.91 × 10 ⁻³	-0.109	0.03120
Standard deviation	0.486	1.143	0.581	0.890	0.399	0.335	0.947	0.641
Probability	0.718	0.956	0.274	0.438	0.265	0.844	0.053	0.897
Freundlich								
K_F (mg g ⁻¹ (mg L ⁻¹) ^{-1/n})	3.41 ± 0.5	4.47 ± 0.7	15.37 ± 0.8	16.2 ± 0.7	3.52 ± 0.3	5.12 ± 0.5	11.7 ± 0.6	12.6 ± 0.8
n	3.03 ± 0.2	2.60 ± 0.3	3.90 ± 0.4	4.18 ± 0.5	2.58 ± 0.1	2.62 ± 0.1	2.74 ± 0.2	2.83 ± 0.2
R^2	0.9120	0.9372	0.9516	0.8687	0.9802	0.9744	0.9547	0.9489
Average of residuals	0.116	0.1716	0.2356	0.164	0.07590	0.1229	0.3523	0.327
Standard deviation	1.30	1.67	3.53	3.58	0.786	1.19	4.29	3.44
Probability	0.558	0.319	0.383	0.064	0.733	0.293	0.556	0.455
Sips								
Q_{\max} (mg g ⁻¹)	13.2 ± 0.6	22.7 ± 0.8	53.0 ± 0.7	41.5 ± 0.8	24.0 ± 0.9	29.9 ± 0.8	76.5 ± 0.7	61.3 ± 0.9
K_S ((mg L ⁻¹) ^{-1/n})	0.178 ± 0.01	0.163 ± 0.02	0.139 ± 0.009	0.307 ± 0.03	0.0882 ± 0.001	0.0763 ± 0.006	0.0464 ± 0.005	0.0916 ± 0.007
n	0.958 ± 0.04	1.17 ± 0.2	1.07 ± 0.1	0.995 ± 0.06	1.24 ± 0.01	1.04 ± 0.06	1.00 ± 0.05	1.01 ± 0.04
R^2	0.9878	0.9733	0.9989	0.9919	0.9969	0.9981	0.9978	0.9982
Average of residuals	0.0269	0.0424	-8.81 × 10 ⁻³	0.0435	-0.0376	3.91 × 10 ⁻³	-0.108	0.0376
Standard deviation	0.483	1.096	0.530	0.890	0.309	0.329	0.947	0.640
Probability	0.628	0.872	0.896	0.468	0.224	0.203	0.052	0.921
Redlich–Peterson								
K_{RP} (L g ⁻¹)	2.46 ± 0.4	4.12 ± 0.4	6.97 ± 0.4	13.3 ± 0.8	1.87 ± 0.3	2.23 ± 0.1	3.55 ± 0.1	5.52 ± 0.1
a_{RP} (mg L ⁻¹) ^{-β}	0.184 ± 0.08	0.300 ± 0.07	0.149 ± 0.1	0.332 ± 0.02	0.147 ± 0.05	0.0858 ± 0.02	0.0464 ± 0.001	0.0904 ± 0.002
g	0.999 ± 0.06	0.895 ± 0.05	0.977 ± 0.01	0.990 ± 0.07	0.890 ± 0.05	0.9732 ± 0.03	1.00 ± 0.001	1.00 ± 0.002
R^2	0.9876	0.9740	0.9989	0.9920	0.9958	0.9981	0.9978	0.9982
Average of residuals	0.0395	0.04286	-0.0267	0.0568	-0.0641	2.89 × 10 ⁻³	-0.109	0.0312
Standard deviation	0.486	1.082	0.537	0.883	0.356	0.327	0.947	0.641
Probability	0.717	0.809	0.690	0.212	0.205	0.183	0.053	0.897

Conditions: temperature was fixed at 25 °C, pH 2.0, adsorbent dosages 5.0 g L⁻¹ and contact time was fixed at 24 h.

and Redlich–Peterson isotherm models closely agreed with the Langmuir isotherm model (see Fig. 9).

From Table 5 it was observed that the maximum biosorption capacity for HRR dye was significantly higher than the biosorption of NRR dye for all the four biosorbents employed. Also it was observed that the maximum biosorption capacities in decreasing order was A–PW > Cr–A–PW > Cr–PW > PW, for both dyes (NRR and HRR). This was exactly the increasing order of the zero charge pH for these biosorbents (see Table 1),

reinforcing the hypothesis of the electrostatic mechanism of biosorption, already discussed above. In addition to this mechanism, the average pore volume and the specific surface area of the biosorbents should play an important role on the biosorption of the dyes since these parameters were significantly increased for Cr–PW and Cr–A–PW when compared to PW (see Table 1). This fact associated with the zero charge potential (pH), explains the higher biosorption capacities of Cr–PW and Cr–A–PW in relation to PW, for biosorption of both NRR and HRR dyes.

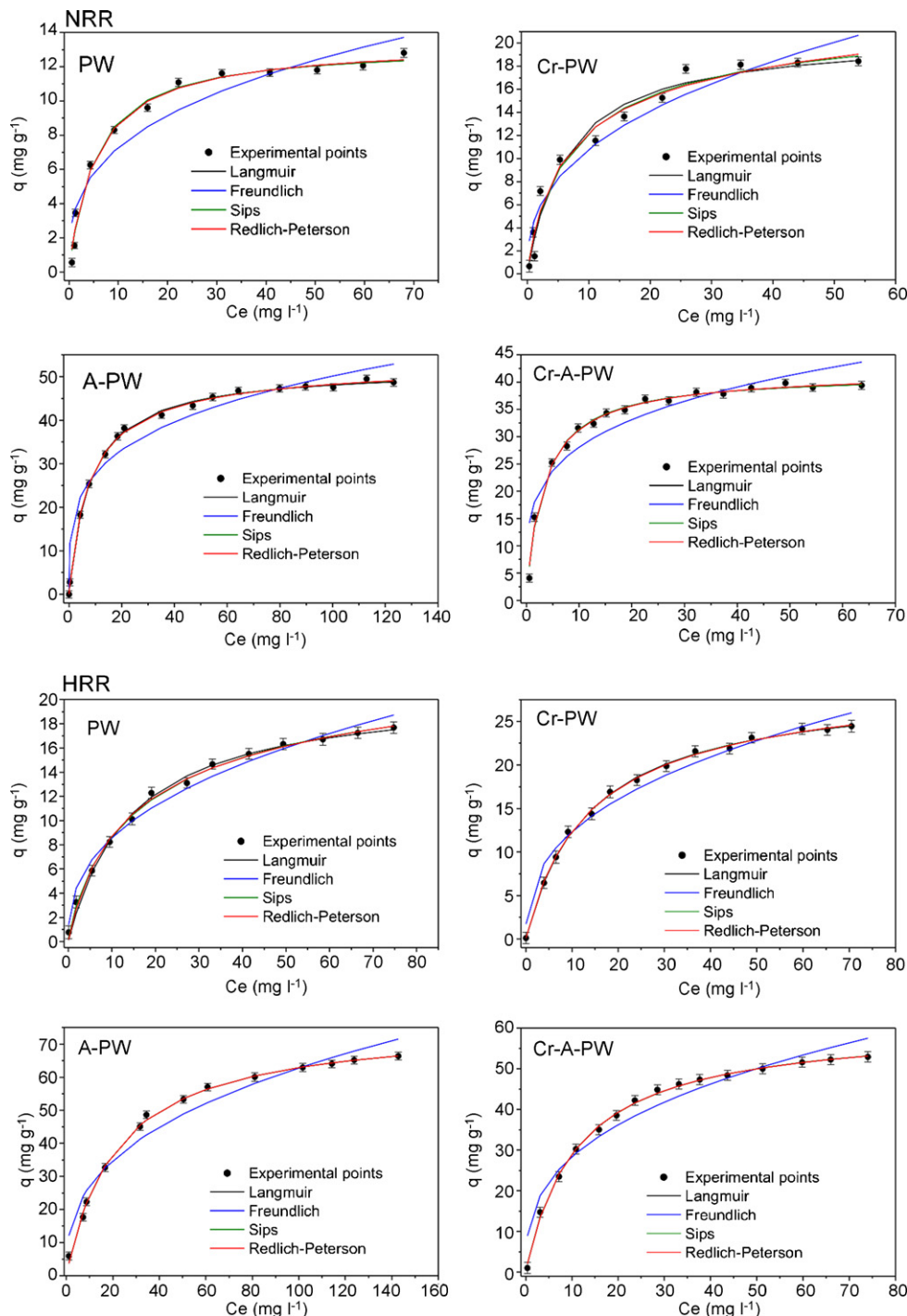


Fig. 9. Biosorption isotherm models for NRR and HRR uptake from aqueous solutions using the biosorbents and the batch biosorption procedure at 25 °C, pH 2.0, biosorbent dosage of 5.0 g L⁻¹, and a contact time of 24 h.

Also, it was already reported [21] that the chromium presented in the chromium loaded Brazilian pine-fruit shell was strongly adhered to piñon fiber, and this element was present in the oxidation state of +3, since Cr(VI) is reduced to Cr(III) by the biomass, as early reported [21,43]. The amount of Cr(III) linked to piñon fiber using a initial concentration of 500.0 mg l⁻¹ of dichromate solution was about 80.0 mg g⁻¹, and the reduced Cr(III) linked to the biosorbent was not released to the aqueous solution under the batch adsorption conditions, as early reported [21]. Considering that the electrostatic mechanism of biosorption, the Cr–PW and Cr–A–PW, should present a surface of the fiber with more positive charges available due to the presence of Cr(III) species, therefore, it is expected that these low-cost adsorbents would present higher adsorption capacities than the unmodified Brazilian pine-fruit shell (PW).

4. Conclusions

The Brazilian pine-fruit shell is a locally available and low cost material that can be used as an alternative biosorbent for successfully removal the reactive dyes in non-hydrolyzed (NRR) and hydrolyzed form (HRR) from aqueous solutions. The biosorption capacity of the Brazilian pine-fruit shell for dyes containing sulfonic groups such as reactive ones could be improved by performing a chemical treatment of the piñon fiber with acid. Alternatively, the biosorption capacity of Brazilian pine-fruit shell could be improved by a treatment with chromium. It should be stressed that large amount of chromium loaded Brazilian pine-fruit shell are generated in Cr(VI) effluent treatment plants by Brazilian pine-fruit shell [21]. Therefore, this work proposes an ecologically correct application of chromium loaded Brazilian pine-fruit shell for dye removal from aqueous effluent.

Acknowledgements

The authors are grateful to Ministério de Ciência e Tecnologia (MCT), and to Conselho Nacional de Desenvolvimento Científico e Tecnológico (CNPq) for financial supports and fellowships. We are grateful to Centro de Microscopia Eletrônica (CME-UFRGS) for the use of the SEM microscope. We also thank to PerkinElmer for donating impact beads utilized in the nebulizer of Analyst 200 spectrometer.

References

- [1] E. Matyjas, E. Rybicki, Novel reactive red dyes, *Autex Res. J.* 3 (2003) 90–95.
- [2] R.O.A. de Lima, A.P. Bazo, D.M.F. Salvadori, C.M. Rech, D.P. Oliveira, G.A. Umbuzeiro, Mutagenic and carcinogenic potential of a textile azo dye processing plant effluent that impacts a drinking water source, *Mutat. Res.* 626 (2007) 53–60.
- [3] D.T. Sponza, Toxicity studies in a chemical dye production industry in Turkey, *J. Hazard. Mater.* 138 (2006) 438–447.
- [4] F.A. Pavan, Y. Gushikem, A.S. Mazzocato, S.L.P. Dias, E.C. Lima, Statistical Design of Experiments as a tool for optimizing the batch conditions to methylene blue biosorption on yellow passion fruit and mandarin peels, *Dyes Pigments* 72 (2007) 256–266.
- [5] A.R. Dinçer, Y. Günes, N. Karakaya, E. Günes, Comparison of activated carbon and bottom ash for removal of reactive dye from aqueous solution, *Bioresour. Technol.* 98 (2007) 834–839.
- [6] R.L. Tseng, S.K. Tseng, F. Wu, Preparation of high surface area carbons from Corn cob with KOH etching plus CO₂ gasification for the adsorption of dyes and phenols from water, *Colloids Surf. A* 279 (2006) 69–78.
- [7] J.J.M. Órfão, A.I.M. Silva, J.C.V. Pereira, S.A. Barata, I.M. Fonseca, P.C.C. Faria, M.F.R. Pereira, Adsorption of a reactive dye on chemically modified activated carbons—influence of pH, *J. Colloid Interface Sci.* 296 (2006) 480–489.
- [8] Y.S. Ho, W.T. Chiu, C.C. Wang, Regression analysis for the sorption isotherms of basic dyes on sugarcane dust, *Bioresour. Technol.* 96 (2005) 1285–1291.
- [9] Z. Aksu, Application of biosorption for the removal of organic pollutants: a review, *Process Biochem.* 40 (2005) 997–1026.
- [10] P. Janos, H. Buchtová, M. Rýznarová, Sorption of dyes from aqueous solutions onto fly ash, *Water Res.* 37 (2003) 4938–4944.
- [11] W. Chu, Dye removal from textile dye wastewater using recycled alum sludge, *Water Res.* 35 (2001) 3147–3152.
- [12] G. Atun, G. Hisarli, W.S. Sheldrich, M. Muhler, Adsorptive removal of methylene blue from colored effluents on fuller's earth, *J. Colloid Interface Sci.* 261 (2003) 32–39.
- [13] M.A. Al-Ghouti, M.A.M. Kraisheh, S.J. Allen, M.N. Ahmad, The removal of dyes from textile wastewater: a study of physical characteristics and adsorption mechanisms of diatomaceous earth, *J. Environ. Manage.* 69 (2003) 229–238.
- [14] M.T. Sulak, E. Demirbas, M. Kobya, Removal of Astrazon Yellow 7GL from aqueous solutions by adsorption onto wheat bran, *Bioresour. Technol.* 98 (2007) 2590–2598.
- [15] F.A. Pavan, E.C. Lima, S.L.P. Dias, A.C. Mazzocato, Methylene blue biosorption from aqueous solutions by yellow passion fruit waste, *J. Hazard. Mater.*, in press. doi:10.1016/j.jhazmat.2007.05.023.
- [16] R. Sivaraj, C. Namasivayam, K. Kadirvelu, Orange peel as an adsorbent in the removal of Acid violet 17 (acid dye) from aqueous solutions, *Waste Manage.* 21 (2001) 105–110.
- [17] A.E. Ofomaja, Kinetics and mechanism of methylene blue sorption onto palm kernel fibre, *Process Biochem.* 42 (2007) 16–24.
- [18] R. Gong, Y. Ding, M. Li, C. Yang, H. Liu, Y. Sun, Utilization of powdered peanut hull as biosorbent for removal of anionic dyes from aqueous solution, *Dyes Pigments* 64 (2005) 187–192.
- [19] T.S. Trung, Chuen-How Ng, W.F. Stevens, Characterization of decrystallized chitosan and its application in biosorption of textile dyes, *Biotechnol. Lett.* 25 (2003) 1185–1190.
- [20] Z. Aksu, S. Tezer, Biosorption of reactive dyes on the green alga *Chlorella vulgaris*, *Process Biochem.* 40 (2005) 1347–1361.
- [21] J.L. Brasil, R.R. Ev, C.D. Milcharek, L.C. Martins, F.A. Pavan, A.A. dos Santos Jr., S.L.P. Dias, J. Dupont, C.P.Z. Noreña, E.C. Lima, Statistical design of experiments as a tool for optimizing the batch conditions to Cr(VI) biosorption on *Araucaria angustifolia* wastes, *J. Hazard. Mater.* 133 (2006) 143–153.
- [22] E.C. Lima, B. Royer, J.C.P. Vaghetti, J.L. Brasil, N.M. Simon, A.A. dos Santos Jr., F.A. Pavan, S.L.P. Dias, E.V. Benvenuti, E.A. da Silva, Adsorption of Cu(II) on *Araucaria angustifolia* wastes: determination of the optimal conditions by statistic design of experiments, *J. Hazard. Mater.* 140 (2007) 211–220.
- [23] J.C.P. Vaghetti, M. Zat, K.R.S. Bentes, L.S. Ferreira, E.V. Benvenuti, E.C. Lima, 4-Phenylenediaminepropylsilica xerogel as a sorbent for copper determination in waters by slurry-sampling ETAAS, *J. Anal. Atom. Spectrom.* 18 (2003) 376–380.
- [24] L.T. Arenas, J.C.P. Vaghetti, C.C. Moro, E.C. Lima, E.V. Benvenuti, T.M.H. Costa, Dabco/silica sol—gel hybrid material. The influence of the morphology on the CdCl₂ adsorption capacity, *Mater. Lett.* 58 (2004) 895–898.
- [25] E.C. Lima, F.J. Krug, A.T. Ferreira, F. Barbosa Jr., Tungsten–rhodium permanent chemical modifier for cadmium determination in fish slurries by electrothermal atomic absorption spectrometry, *J. Anal. Atom. Spectrom.* 14 (1999) 269–274.

- [26] L. Prosky, N.G. Asp, T. Schweizer, J.W. De Vries, I. Furda, Determination of insoluble and soluble dietary fiber in food and food products: collaborative study, *J. AOAC Int.* 75 (1992) 360–367.
- [27] J.S. Noh, J.A. Schwarz, Effect of HNO₃ treatment on the surface acidity of activated carbons, *Carbon* 28 (1990) 675–682.
- [28] C.G. Passos, F. Ribaski, N.M. Simon, A.A. dos Santos Jr., J.C.P. Vaghetti, E.V. Benvenuti, E.C. Lima, Use of statistical design of experiments to evaluate the sorption capacity of 7-amine-4-azaheptylsilica and 10-amine-4-azadecylsilica for Cu(II), Pb(II) and Fe(III) adsorption, *J. Colloid Interface Sci.* 302 (2006) 396–407.
- [29] D.L. Pavia, G.M. Lampman, G.S. Kriz, *Introduction to Spectroscopy*, 2nd edition, Saunders Golden Sunburst Series, New York, 1996.
- [30] F.A. Pavan, I.S. Lima, E.C. Lima, C. Airoidi, Y. Gushikem, Use of ponkan mandarin peels as biosorbent for toxic metals uptake from aqueous solutions, *J. Hazard. Mater.* 137 (2006) 527–533.
- [31] J.D. Roberts, M.C. Caserio, *Basic Principles of Organic Chemistry*, 2nd edition, Benjamin Incorporation, London, W.A., 1977.
- [32] K.V. Kumar, K. Porkodi, Mass transfer, kinetics and equilibrium studies for the biosorption of methylene blue using *Paspalum notatum*, *J. Hazard. Mater.* 146 (2007) 214–226.
- [33] S. Largegren, About the theory of so-called adsorption of soluble substances, *Kungliga Suensk Vetenskapsakademiens Handlingar* 24 (1898) 1–39.
- [34] Y.S. Ho, G.M. McKay, Pseudo-second order model for sorption process, *Process Biochem.* 34 (1999) 451–465.
- [35] Weber-F W.J. Jr., J.C. Morris, Kinetics of adsorption on carbon from solution, *J. Sanit. Eng. Div. Am. Soc. Civil Eng.* 89 (1963) 31–59.
- [36] F.A. Pavan, S.L.P. Dias, E.C. Lima, E.V. Benvenuti, Removal of Congo red from aqueous solution by anilinepropylsilica xerogel, *Dyes Pigments* 76 (2008) 64–69.
- [37] W.H. Cheung, Y.S. Szeto, G. McKay, Intraparticle diffusion processes during acid dye adsorption onto chitosan, *Bioresour. Technol.* 98 (2007) 2897–2904.
- [38] C.G. Passos, E.C. Lima, L.T. Arenas, N.M. Simon, B.M. da Cunha, J.L. Brasil, T.M.H. Costa, E.V. Benvenuti, Use of 7-amine-4-azaheptylsilica and 10-amine-4-azadecylsilica xerogels as adsorbent for Pb(II) Kinetic and equilibrium study, *Colloids Surf. A.*, in press, doi:10.1016/j.colsurfa.2007.09.025.
- [39] I. Langmuir, The adsorption of gases on plane surfaces of glass, mica and platinum, *J. Am. Chem. Soc.* 40 (1918) 1361–1403.
- [40] H.M.F. Freundlich, Über die adsorption in lösungen, *Zeitschrift für Physikalische Chemie (Leipzig)* 57A (1906) 385–470.
- [41] R. Sips, On the structure of a catalyst surface, *J. Chem. Phys.* 16 (1948) 490–495.
- [42] O. Redlich, D.L. Peterson, A useful adsorption isotherm, *J. Phys. Chem.* 63 (1959) 1024–1027.
- [43] H.S. Altundogan, Cr(VI) removal from aqueous solution by iron(III) hydroxide-loaded sugar beet pulp, *Process Biochem.* 40 (2005) 1443–1452.